Online Supplement for *High-speed microjets issue from bursting oil gland reservoirs of citrus fruit*

1 Supplementary Movie Captions

Movie S1: Video sequence of oil jetting for all citrus species tested. (*Citrus sinensis* slowed 83x. *Citrus aurantifolia, Citrus paradisi, Citrus limon,* and *Citrus reticulata* slowed 133x.)

Movie S2: Cross-sectional view of Florida navel orange peel bending to the point of jetting. The albedo is compressed while the outer layer, or flavedo, experiences tension. (slowed 133x)

Movie S3: An orange oil jet undergoing the transition from jetting to dripping. (slowed 266x)

Movie S4: Comparison of jet instability witnessed in natural (slowed 233x) and artificial (slowed 533x) orifices.

2 Supplementary Figures and Table

We include supplementary figures to support the assertion that oil gland size and fruit size are independent.

Table S1: Fitting parameter data corresponding to the curves in **Fig.S4**, of the form $V_0 = mE_{\mathrm{fl}}^n$.

Fit Type	*Day 1*	*Day 8*	*Day 15*
Exp. Fit			
m	*2.543*	*2.291*	*4.011*
n	*0.2671*	*0.2979*	*0.1977*
R^2	*0.9689*	*0.9480*	*0.4390*
Model Fit			
m	2.752	2.901	3.093
n	0.2500	0.2500	0.2500
R^2	0.9652	0.9331	0.4094

www.pnas.org/cgi/doi/10.1073/pnas.1720809115

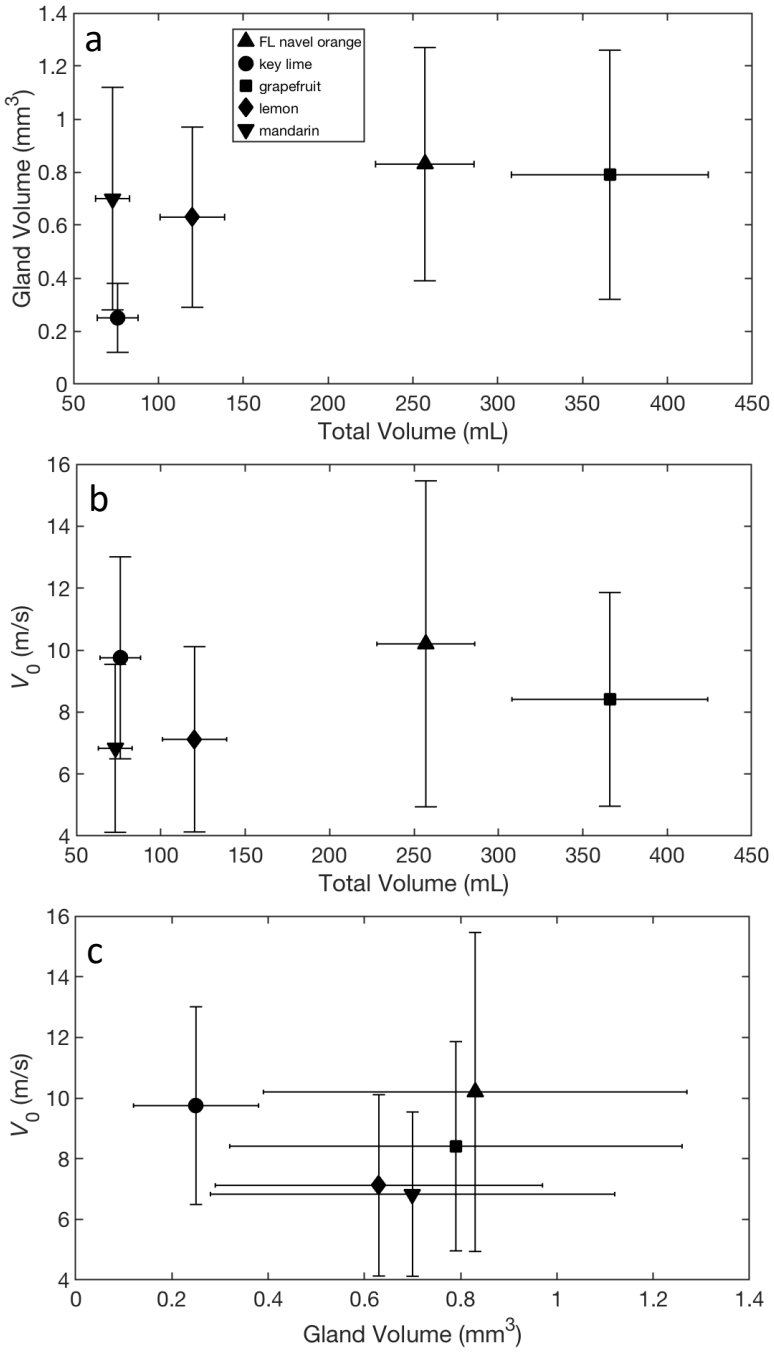

Figure S1: **(a)** The relation between gland volume (N= 100 for each species) and bulk fruit volume (N= 30 for each species). **(b)** The relation between jet exit velocity (N= 100 for each species) and bulk fruit volume. **(c)** The relation between jet exit velocity and oil gland reservoir volume.

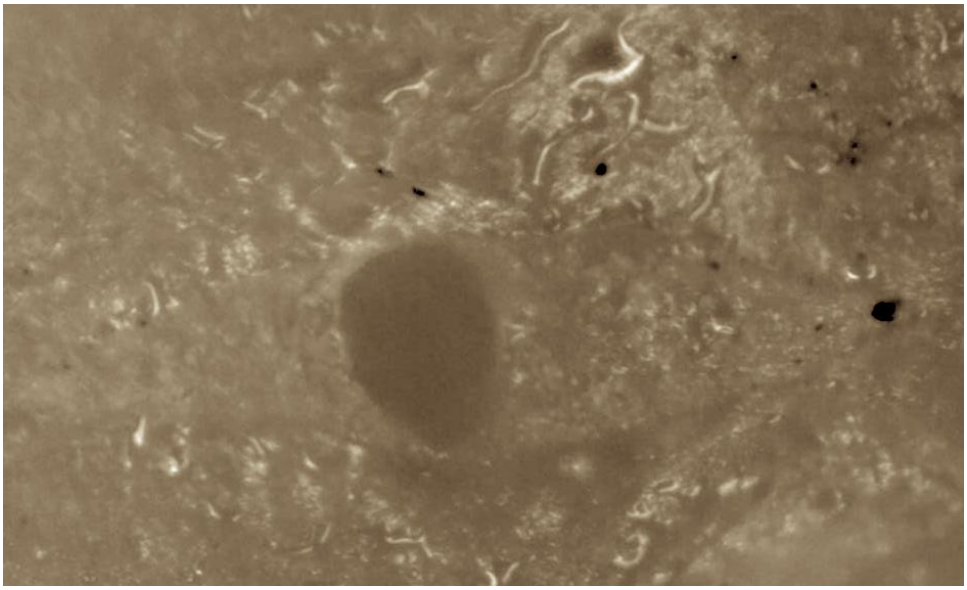

Figure S2: Photograph showing a torn flavedo revealing a jet orifice, looking down into the reservoir. Glossy regions are residual oil. The opening measures roughly 100 μm in diameter.

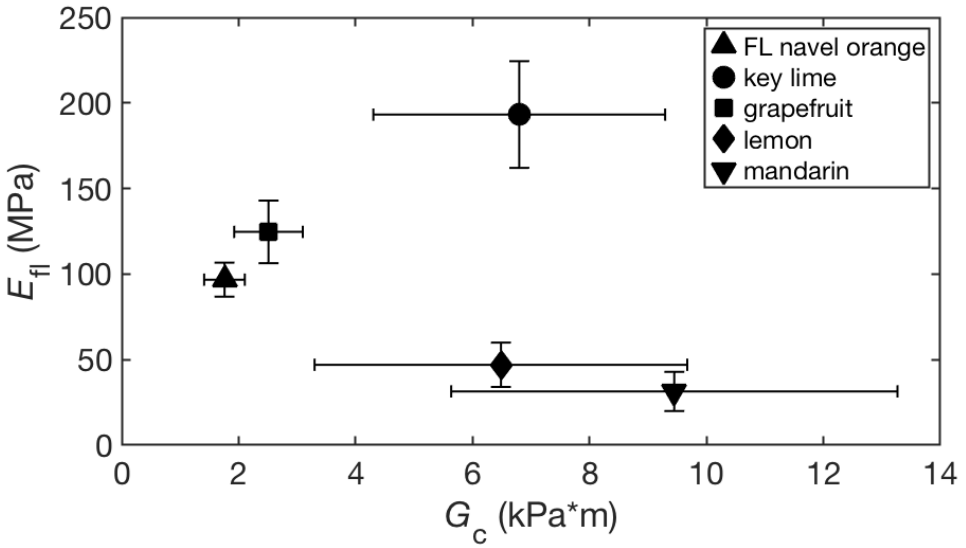

Figure S3: The relation between flavedo stiffness E_{fl} (N= 5 for each species) and strain energy release rate G_{c} (N= 5 for each species,).

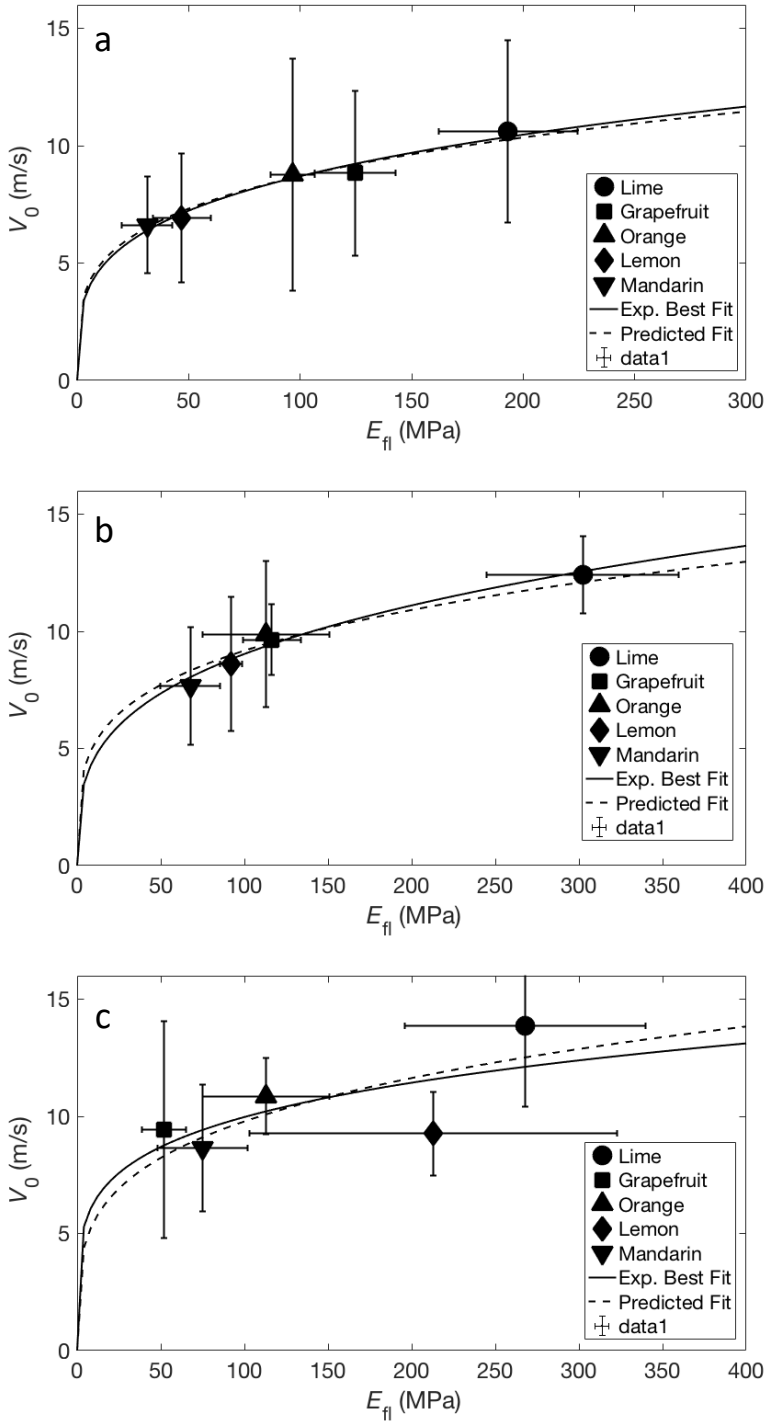

Figure S4: The relation between flavedo stiffness E_{fl} (N= 5 for each species) and jet exit velocity V_0 (N= 9 for each species) **(a)** 1, **(b)** 8, and **(c)** 15 days following purchase. Fitting parameters for the curves in plots (a)-(c) are provided in **Table S1**.

3 Citrus jet instability

While some jet ports below the cracked flavedo photographed in this study are nearly perfect circles, others are not. Free jets experience capillary instability and break up even when orifices are perfectly circular, the fluid is inviscid, and flow is laminar[1]. Previous studies show that jet stability is influenced by inlet conditions and orifice geometry[2–4], and that asymmetric jets are less stable, encouraging breakup. The orifice geometry through which citrus jets issue is often elliptical in nature, and at times shrouded by irregular edges of the torn flavedo. We measure 10 such orifices and find they have an eccentricity range of $\epsilon = \sqrt{1 - b^2/a^2} = 0.33 - 0.99$, and hydraulic diameter of $D_h = 114$ μm on average. As witnessed with elliptical jets, the citrus oil exhibits major and minor axes switching (Movie S4), a consequence of initial perturbations in the jet imposed by eccentric orifices.

Instability in citrus jets may be classified into two breakup regimes, driven by jet velocity V_0. The initial breakup regime of Rayleigh instability begins when the liquid Weber number $\mathrm{We} = \rho V_0^2 D_h/\gamma > 8$, resulting in $V_0 > 1.6$ m/s, also signaling the transition from dripping to jetting[5] (Movie S3). The end of the Rayleigh breakup regime occurs when $\mathrm{We} > 137$, corresponding to $V_0 > 6.6$ m/s, and triggering entrance into the first wind induced breakup regime. Citrus jets regularly pass this issuance velocity resulting in unpredictable breakup distances. Another source of instability is the ragged office perimeters produced by the non-uniform tearing the citrus flavedo upon jet issuance, as seen in **Fig.S5**. The longest breakup distances we observe from citrus peels approach 2 mm, far shorter than we were able to create artificially using orange oil shot through needles with $D_h = 160$ μm (Movie S4).

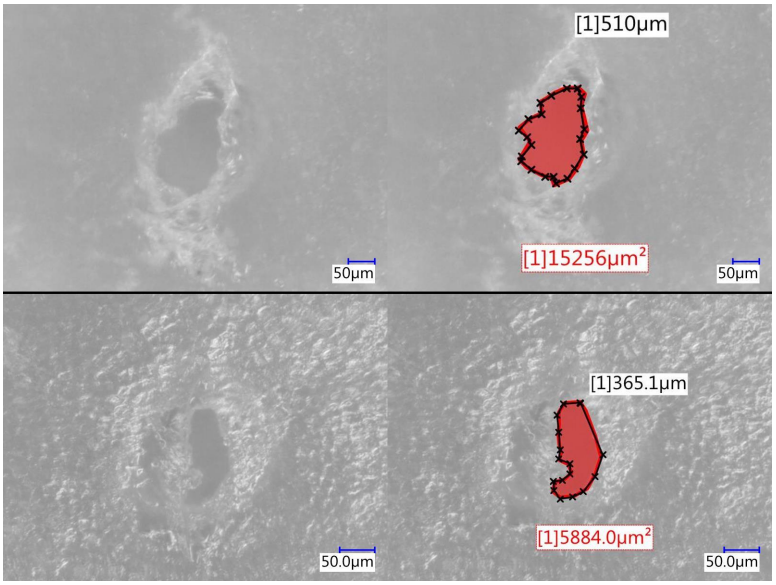

Figure S5: Orifice shapes following two jetting events, with the orifice accentuated in red in the righthand panels.

References

[1] Rayleigh, L., 1878 On the instability of jets. *Proceedings of the London Mathematical Society* **1**, 4–13.

[2] Blaisot, J. & Adeline, S., 2003 Instabilities on a free falling jet under an internal flow breakup mode regime. *International Journal of Multiphase Flow* **29**, 629–653.

[3] Amini, G. & Dolatabadi, A., 2012 Axis-switching and breakup of low-speed elliptic liquid jets. *International Journal of Multiphase Flow* **42**, 96–103.

[4] Amini, G. & Dolatabadi, A., 2011 Capillary instability of elliptic liquid jets. *Physics of Fluids* **23**, 084109.

[5] van Hoeve, W., Gekle, S., Snoeijer, J. H., Versluis, M., Brenner, M. P. & Lohse, D., 2010 Breakup of diminutive Rayleigh jets. *Physics of Fluids* **22**.